

# Photo-Catalytic Degradation for Organic Removal from Iraqi-Oilfield Wastewater Produced: Experimental, Optimization, Kinetic and Economic Insights Study

Liqaa Tareq Hadi<sup>1</sup>, Awad E. Mohammed<sup>2</sup>, Raid T. Al-khateeb<sup>3</sup>, Ali A. Hassan<sup>3,4</sup>, Jasim I. Humadi<sup>5\*</sup>, Muataz A. Hammadi<sup>6</sup> and Amer T. Nawaf<sup>5</sup>

<sup>1</sup>ICT Department, AL-Furat Al-Awsat Technical University, Muthanna, Iraq

<sup>2</sup>AL-Hawija Technical College, Northern Technical University, Mosel, Iraq.

<sup>3</sup>Chemical Department, College of Engineering, University of Muthanna, Muthanna, Iraq

<sup>4</sup>College of Engineering, Al Ayen University, Nasiriyah, 64001, Iraq

<sup>5</sup>Petroleum and Gas Refinery Engineering Department, College of Petroleum Process Engineering, Tikrit University, Tikrit, Iraq.

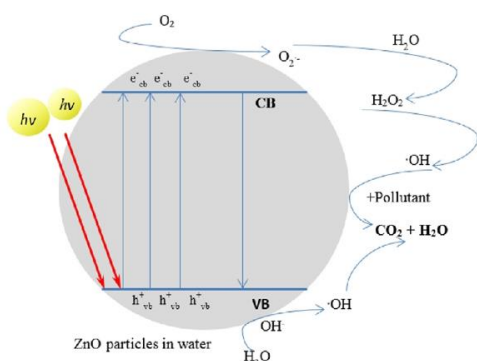
<sup>6</sup>College of Administration and Economics, Al-Iraqia University, Baghdad, Iraq

Received: 03/06/2025, Accepted: 05/11/2025, Available online: 16/12/2025

\*to whom all correspondence should be addressed: e-mail: [jasim\\_alhashimi\\_ppe@tu.edu.iq](mailto:jasim_alhashimi_ppe@tu.edu.iq)

<https://doi.org/10.30955/gnj.07726>

## Graphical abstract



## Abstract

Globally, large volumes of oily wastewater can be produced due to the industrial developments in petrochemicals, oil and gas, food, and pharmaceutical sectors which can be affected directly on the ground water and drinking water resources. Therefore, it is very necessary treating the injected water into oil reservoirs in order to reduce the formation damage. Photo-catalytic technique can be used to reduce the oil droplets in the produced wastewater of Iraqi-oilfield. In this study, a heterogeneous photo-catalysis process was conducted using (ZnO, TiO<sub>2</sub> and Al<sub>2</sub>O<sub>3</sub>) as a catalytic materials and UV lamps photo as a source of energy to optimize wastewater degradation under different operating conditions of irradiation time (30-120 minute), pH (3-9), catalyst dose (0.25-1 g), UV lamps (2-8 A). This study was presented new integrated photo-catalysis strategy for purification of industrial wastewater under mild operational conditions

and cost effective process. The Mini tab with Response Surface Methodology was used here to validate the experimental results. Based on the results obtained in this work it was observed that the organic removal of oil droplets in photo-catalytic degradation were 98.2% and 92.5%, 88.9% for ZnO, TiO<sub>2</sub> and Al<sub>2</sub>O<sub>3</sub> respectively under the optimum operating conditions of time (120 minute), pH (9), catalyst dose (1 g), UV lamps (8 A). The kinetic study results for photo-catalytic reaction under using ZnO were followed pseudo-first order with  $0.0032 \text{ min}^{-1}$  at ( $R^2=0.94$ ). Finally, it can be concluded that the photo-catalytic degradation process was an efficient in oil droplet removal from water within using ZnO catalyst as compared with others.

**Keywords:** Photo-catalytic Degradation. Oil droplet, Oily wastewater treatment, catalyst ZnO

## 1. Introduction

Refinery processes converts the crude oil to valuable products such as petroleum and huge amounts of by-products of wastewater up to 0.4 to 1.6 times of the crude oil volume processes (Ali A. Hassan *et al.* 2019; A. S. Anitha *et al.* 2024). The wastewater produced consists of various complex compositions of organic and inorganic compounds, the majority of these are phenols, salts, emulsified oils and organic acids (M. K. Ibrahim *et al.* 2019; Y. Zang *et al.* 2024). Oil and grease from these compounds composed from fatty acids and hydrocarbons which imposed more legislations for discharge (Ahmed *et al.* 2021). Therefore, to face the strict regulations and reuse the wastewater produced, it is very necessary to oily saline wastewater (Ali Abed Hassan & Shakir 2024). Many efforts by researchers were focused on treating oily

Liqaa Tareq Hadi, Awad E. Mohammed, Raid T. Al-khateeb, Ali A. Hassan, Jasim I. Humadi, Muataz A. Hammadi, Amer T. Nawaf (2025), Photo-Catalytic Degradation for Organic Removal from Iraqi-Oilfield Wastewater Produced: Experimental, Optimization, Kinetic and Economic Insights Study, *Global NEST Journal*, **28**(1), 07726.

**Copyright:** © 2025 Global NEST. This article is an open access article distributed under the terms and conditions of the Creative Commons Attribution International ([CC BY 4.0](https://creativecommons.org/licenses/by/4.0/)) license.

wastewater produced using conventional methods and reused again in different refining processes. Degradation of aqueous contaminants via conventional techniques include biological, coagulation and flocculation(Ivanenko *et al.* 2020), adsorption and flotation (Saleh Jafer & Hassan 2019).

Despite widespread use of these methods for the residual wastewater treatment , Nevertheless, these techniques are non-destructive, since they just transfer the pollutant from water to solid matrix (Al-Hassan & Shakir 2024). Due to these drawbacks, it was very important to find alternative wastewater treatment techniques, more efficient and friendly. Advanced oxidation process (AOPs) represents the efficient chemical treatment for industrially used based on producing free radicals (-OH) (Alturki *et al.* 2021). AOPs has appeared as a suitable waste water treatment alternative because it has demonstrated rapid degradation of recalcitrant and non-biodegradable compounds in waste water (Naeem *et al.* 2018). Producing more free radicals can be enhanced using high energy electromagnetic waves which improve the efficiency of (AOPs) process(Al-zobai *et al.* 2020).

(AOPs) considers useful, complete oxidation and environment friendly, which can producing unharful of end-products for all types of pollutants (Alabdrraba *et al.* 2020; Atiyah *et al.* 2020; Kamal *et al.* 2020; Mohammed *et al.* 2019; Sh 2020). Photochemical degradation procedures comprise photochemical within UV lamp and heterogeneous (photocatalysis, etc.) processes (Orooji *et al.* 2020). Photocatalytic squalor is one of the many active oxygen producers (AOPs). ZnO, TiO<sub>2</sub>, or CdS are possible catalysts in sophisticated chemical processes (Mohammadi Ziarani *et al.* 2024). Because of its extremely precise surface area, nano-dimensional titanium dioxide allows for orderly charge separation and charge trapping of ions on its surfaces (Ulhaq *et al.* 2021). The oxidative power of the bulk-sized TiO<sub>2</sub> was found to rise with the opacity of the aqueous phase in the demonstration of nano-sized TiO<sub>2</sub> (Gutierrez-Mata *et al.* 2017). **Nawaf *et al.* (2023)** investigated the performance of phenol removal from refinery wastewater Fe<sub>2</sub>O<sub>3</sub>/AC and hydrogen peroxide in digital basket baffle batch reactor. The results proved 95.35% oxidation efficiency under the best process conditions (120 min, 85°C, and 600 rpm) (Nawaf *et al.* 2023). **Khamees *et al.* (2023)** studied the activity of (Fe<sub>2</sub>O<sub>3</sub>- alkaline/TiO<sub>2</sub>) catalyst for wetperoxideoxidation technology of phenol removal. Results showed that maximum oxidation efficiency was 95.931% under 80°C and 90min (Khamees *et al.* 2023). **Issa *et al.* (2025)** examined the efficiency of catalytic wet photo oxidation technology using ZnO/Al<sub>2</sub>O<sub>3</sub>catalyst. Results performed 95.45% phenol oxidation efficiency at 70°C, 100sec, and 750 rpm (Issa *et al.* 2025).

In this study the removal of oily droplets from wastewater produced via photo catalytic oxidation by different catalyst under UV light and compared between them under different operating conditions of time, catalyst dose, UV light lamps and pH. Minitab software with in

Response Surface Methodology was used here validates the experimental results.

## 2. Experimental Methodology

### 2.1. Materials and Chemicals

In this work, all the materials and chemicals were in high purity and analytical grade without further purification. These chemicals were zinc oxide (ZnO, purity 99.9%), titanium dioxide (TiO<sub>2</sub>, purity 99.9%, Sigma Aldrich), aluminum oxide (Al<sub>2</sub>O<sub>3</sub>, purity 99.5%), sodium hydroxide (NaOH, purity 97%), sodium chloride (NaCl, purity 99%), carbon tetra-chloride (CCl<sub>4</sub>, purity 99.5%) and sulfuric acid (H<sub>2</sub>SO<sub>4</sub>, purity 99.9%) was supplied from Sigma Aldrich. Organic droplets as a contaminant component into wastewater were supplied from Iraqi-oil field. Distilled water was used in preparation of solutions in this work.

### 2.2. Preparation of Wastewater Produced

The produced wastewater was prepared by adding organic droplets were supplied from the local Iraqi-oil fields. To break the oil emulsion, 50 mL of generated water in the separating funnel was mixed with 0.25 gram of NaCl. After adding five milliliters of carbon tetrachloride, the mixture was vigorously shaken for two minutes. When the solution divided into two different layers after 20 minutes, the lowest (organic) layer was removed for the absorbance measurement, and concentration was determined using the calibration curve (Ali Abd Hassan & Shakir 2024). In this work, the sample prepared was kept in environmental conditions the same of produced wastewater into the oilfield to obtain the same specifications while using in experiments. The specifications of produced water in this work were characterized and illustrated in **Table 1**. The acidity/basicity function of solution was adjusted with using 1 N H<sub>2</sub>SO<sub>4</sub> or 1 N NaOH was measured via WTWpH-720 digital pH meter to detect the pH of the solutions. A turbid meter (Lovibond, SN 10/1471, Germany) was used to measure and read the turbidity.

**Table 1.** Specifications of Produced Wastewater.

Item	value
Oil density	209.11 (mg/l)
Turbidity	70.5 NTU
pH	6.88
Oxygen content	0.064 (mg/l)
TDS	121040 (mg/l)
Specific gravity	0.995
viscosity	1.03 m Pa/S
iron	0.44 (mg/l)
sulphate	50.1 (mg/l)

### 2.3. Photo-Catalytic Oxidation Procedure

In this work, Photo-Catalytic reactor was used in all the experiments to degrade the produced wastewater as shown in **Figure 1**. As can be seen in **Figure 1**, the UV light was supplied as energy source equipped in with 250 ml three necked flask as a batch reactor contains about 100 ml of the produced wastewater sample. The sample was magnetic stirred with 200 rpm for (30-120 minute) with a certain amounts of catalyst dosage under different

operating conditions. The solution pH value was adjusted using NaOH/H<sub>2</sub>SO<sub>4</sub> before adding the reagents and pH value was measured using Digital Portable Digital pH Meter (PH310P, range: -2.00 - 20.00 pH, accuracy:  $\pm 0.01$  pH, Perlone Medical Equipment Co., Ltd., China). After completing the experiments time under the specified conditions, the final treated water is sampled and tested to evaluate its purity. The operating conditions used in this work with their ranges were degradation time (X<sub>1</sub>), solution pH (X<sub>2</sub>), catalyst dose (X<sub>3</sub>), and UV light (X<sub>4</sub>) as illustrated in **Table 2**. Design of experiments in this work was conducted using Mini Tab software with Surface Methodology.

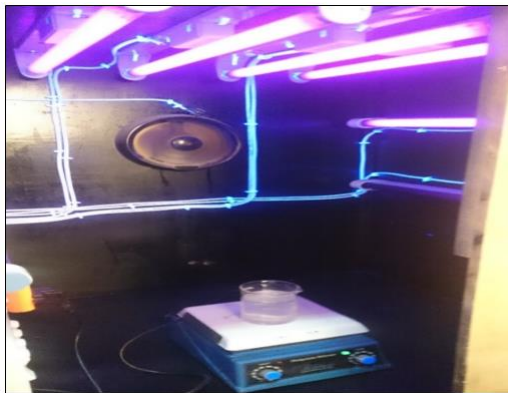


**Figure 1.** Photocatalytic oxidation reactor

**Table 2.** Independent parameters

Limits	Varieties
X <sub>1</sub> : time (min)	30-120
X <sub>2</sub> : pH	3-9
X <sub>3</sub> : Catalyst dose (gm)	0.25-1
X <sub>4</sub> : Current (Amps)	2-8

#### 2.4. Analytical measurements and kinetic study

In all the experiments of photo-catalytic process, the outlet concentration of organic pollutant in the produced wastewater sample was measured utilizing UV spectrophotometer (UV-1800 Shimadzu, Japan). The efficiency of photo-catalytic degradation process for organic contaminant of oil droplets were calculated using the following formula:

$$\eta = \frac{C_o - C_t}{C_o} \times 100\% \quad (1)$$

Where C<sub>o</sub> is the initial concentration of organic contaminant (ppm) in the sample, C<sub>t</sub> is the outlet concentration of organic contaminant in the produced wastewater;  $\eta$  represents the efficiency of photo-catalytic degradation. The kinetic study of the process was estimated here utilizing Langmuir–Hinshelwood kinetics model with pseudo-first order as illustrated in (Eq. (2)). By plotting  $\ln(C_o/C)$  against time for each run.

$$\ln \left[ \frac{C_o}{C} \right] = K_1 t \quad (3)$$

The plotted data can give a straight line with a slope K<sub>1</sub>(min<sup>-1</sup>) represents pseudo-first-order rate constant.

### 3. Results and discussion

#### 3.1. Catalysts Characterizations

##### 3.1.1. Surface area, Pore volume and Pore Size Distribution

The characterization results of surface area, pore volume and pore size distribution for ZnO, TiO<sub>2</sub> and Al<sub>2</sub>O<sub>3</sub> were presented in **Table 3**. It can be seen from **Table 2** the values of surface area for ZnO, TiO<sub>2</sub> and Al<sub>2</sub>O<sub>3</sub> are 13 m<sup>2</sup>/g, 186.5 m<sup>2</sup>/g and 129 m<sup>2</sup>/g respectively. The pore volume tabulated as 3.436 cm<sup>3</sup>/g, 0.36 cm<sup>3</sup>/g and 0.1 cm<sup>3</sup>/g for ZnO, TiO<sub>2</sub> and Al<sub>2</sub>O<sub>3</sub> respectively. The results of average pore size data for the catalysts prepared of ZnO, TiO<sub>2</sub> and Al<sub>2</sub>O<sub>3</sub> are 10 nm, 15 nm and 12 nm respectively. Residence time and operation temperature considers the most important parameters influence on the pore volume characteristics. The high value of surface area is very important in adsorption and kinetics issues, where large surface area enhance the efficiency of degradation process. This parameter is strongly depend on the pore volume characteristic, where an increase or decrease in surface area directly related on the value of pore volume due to the filling of internal pores hence, handling the reaching of N<sub>2</sub>-gas.

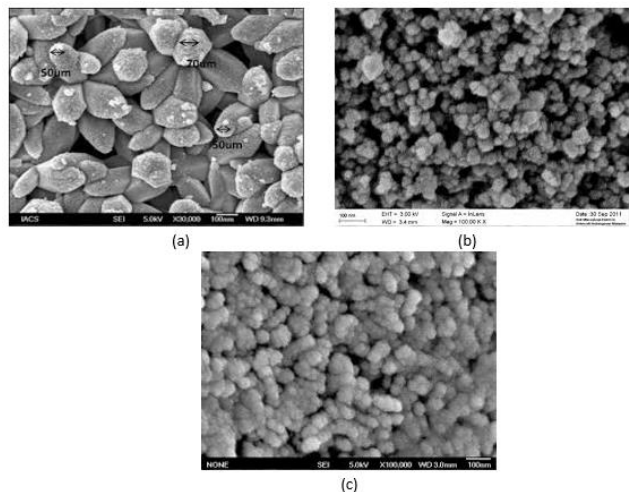


**Figure 2.** FESEM images for (a) ZnO (b) TiO<sub>2</sub> (c) Al<sub>2</sub>O<sub>3</sub>

**Table 3.** The texture properties of the catalysts.

Sample	S <sub>BET</sub> (m <sup>2</sup> /g)	V <sub>t</sub> (cm <sup>3</sup> /g)	D <sub>p</sub> (Å)
ZnO	13	3.436	10
TiO <sub>2</sub>	186.5	0.1	15
Al <sub>2</sub> O <sub>3</sub>	129	0.36	12

##### 3.1.2. FESEM-EDX

In this work, FESEM characterization was conducted at different magnifications to observe the structure and morphology for the catalysts prepared as shown in **Figure 2**. **Figure 2a**, **Figure 2b**, and **Figure 2c** represents the images for ZnO, TiO<sub>2</sub>, Al<sub>2</sub>O<sub>3</sub> respectively. The morphology of the catalyst ZnO can give uniform distribution and homogeneity of the surface. It can be noticed from **Figure 2b**, that the image shows that TiO<sub>2</sub> magnified at X100,000 magnifications indicated microporosity of the catalyst with cracks, cavities, and uniform particle size distribution found on the homogenous surface. Generally, tetania can be exist with in more type of crystalline phase which are rutile (more stable), anatase (more active) and brookite

(Ohara *et al.* 2008). The morphology for  $\text{Al}_2\text{O}_3$  was illustrated in **Figure 2c**, magnified at  $\times 100,000$  magnifications indicated also the microporosity of the catalyst with smaller than  $\text{TiO}_2$  and uniform particle size distribution found on the homogenous surface.

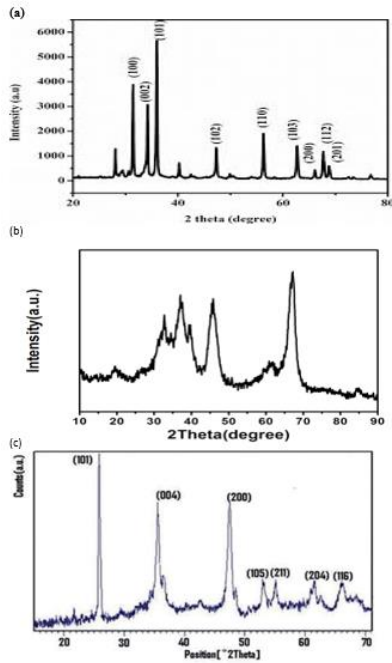


**Figure 3.** XRD spectra for (a)  $\text{ZnO}$  (b)  $\text{TiO}_2$  (c)  $\text{Al}_2\text{O}_3$

### 3.1.3. XRD

The crystallinity of  $\text{ZnO}$ ,  $\text{TiO}_2$ ,  $\text{Al}_2\text{O}_3$  was characterized with in X-ray diffraction spectra in the ranges ( $2\theta = 10^\circ$  to  $2\theta = 80^\circ$ ) as illustrated in **Figure 3**. The spectrum of the surface was presented in **Figure 3**. It can be observed from **Figure 3a**, strong peaks were presented in around  $2\theta = 35.5^\circ$  and  $2\theta = 38^\circ$  attributed to the surface structure of  $\text{TiO}_2$ . Also, it was seen other peaks with low intensities around  $2\theta = 48^\circ$ ,  $2\theta = 58^\circ$ ,  $2\theta = 65^\circ$ ,  $2\theta = 68^\circ$ . These peaks can be assigned to the dispersion of these nano-particles. This indicates a good and uniform distribution of the surface. The

differences in peak intensities observed in **Figure 3b & Figure 3c** were significant due to the amount impregnated for each catalyst especially after impregnated of alkaline materials.

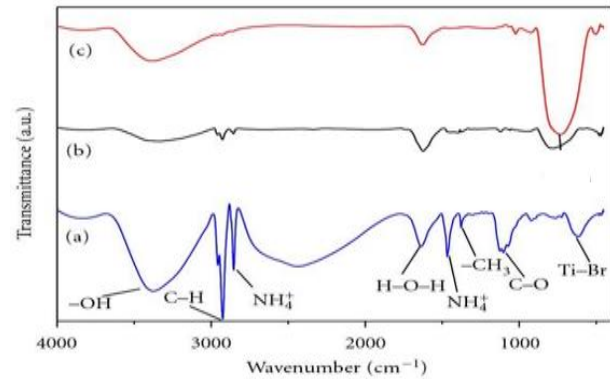


**Figure 4.** FTIR spectra for (a)  $\text{TiO}_2$  (b)  $\text{ZnO}$  (c)  $\text{Al}_2\text{O}_3$

### 3.1.4. FTIR

Characterization of surface chemistry (acid or base functional groups) for the support and catalysts represents more significant for different processes uses. These groups are basic in adsorption, oxidation, and desulfurization process. In this study the FTIR spectra was conducted in the ranges ( $400 - 4000 \text{ cm}^{-1}$ ) for  $\text{ZnO}$ ,  $\text{TiO}_2$ ,  $\text{Al}_2\text{O}_3$  were illustrated in **Figure 4a**, **Figure 4b**, and **Figure 4c** respectively. It can be seen from these figures, several of functional groups were presented on the surface of the support and the catalysts with slightly differences could be seen assigned to the loading amounts of nano-particles for active components. A wide ranges of spectra could be observed in these figures from  $1010$  and  $500 \text{ cm}^{-1}$  are attributed to C-H for alkene aromatic rings (Srivastava *et al.* 2006). The bands appeared in the spectra of  $1150$  to  $1300 \text{ cm}^{-1}$  assigned to the C-O for esters, phenols, and alcohols (Zawadzki 1989). The spectra ranges of  $1650$  to  $1500 \text{ cm}^{-1}$  attributed to aromatic and carboxyl structures (El-Hendawy 2006).

**Table 4.** Results of the BBD experiments

NO	Time (min) X <sub>1</sub>	pH X <sub>2</sub>	Dose (gm) X <sub>3</sub>	UV lamps X <sub>4</sub>	Organic removal by $\text{Al}_2\text{O}_3$ (%)	Organic removal by $\text{TiO}_2$ (%)	Organic removal by $\text{ZnO}$ (%)
1	30	3	0.625	5	62.4	68.5	73.5
2	120	3	0.625	5	69.1	75.4	80.4
3	30	9	0.625	5	71.5	77.4	82.6
4	120	9	0.625	5	78.9	83.1	88.5
5	75	6	0.25	2	60.5	65.3	70.5
6	75	6	1	2	77.9	81.5	86.3
7	75	6	0.25	8	66.4	72.5	79.4
8	75	6	1	8	85.3	90.2	96.5
9	30	6	0.625	2	73.5	78.2	85.3
10	120	6	0.625	2	80.5	84.6	89.5
11	30	6	0.625	8	84.9	88.9	93.6
12	120	6	0.625	8	88.9	92.5	97.8
13	75	3	0.25	5	63.1	77.5	85.2
14	75	9	0.25	5	73.2	78.5	84.9
15	75	3	1	5	78.5	82.5	88.9
16	75	9	1	5	87.9	92.5	98.2
17	30	6	0.25	5	67.3	72.5	77.4
18	120	6	0.25	5	73.5	78.1	84.6

19	30	6	1	5	77.8	81.9	86.4
20	120	6	1	5	86.5	88.9	93.6
21	75	3	0.625	2	73.9	78.4	84.3
22	75	9	0.625	2	73.1	77.5	84.9
23	75	3	0.625	8	76.5	81.8	86.4
24	75	9	0.625	8	86.3	90.5	94.9
25	75	6	0.625	5	82.5	86.4	90.5
26	75	6	0.625	5	83	85.9	91
27	75	6	0.625	5	82.9	86.9	90.2

**Table 5.** ANOVA Examination of Organic Removal Using ZnO.

Foundation	DOF	Seq. SS	Adj. MS	Fisher Value	P-test Value
1-Model	14	915.61	65.401	2.33	0.075
Linear	4	801.42	200.356	7.14	0.003
$X_1$	1	105.61	105.613	3.77	0.076
$X_2$	1	109.81	109.807	3.92	0.071
$X_3$	1	395.6	395.601	14.11	0.003
$X_4$	1	190.4	190.403	6.79	0.023
Square	4	69.82	17.454	0.62	0.655
$X_1^2$	1	35.36	35.363	1.26	0.283
$X_2^2$	1	33.67	33.667	1.2	0.295
$X_3^2$	1	36.4	36.401	1.3	0.277
$X_4^2$	1	1.61	1.613	0.06	0.814
2-Way Interaction	6	44.36	7.394	0.26	0.944
$X_1 * X_2$	1	0.25	0.25	0.01	0.926
$X_1 * X_3$	1	0	0	0	1
$X_1 * X_4$	1	0	0	0	1
$X_2 * X_3$	1	28.09	28.09	1	0.337
$X_2 * X_4$	1	15.6	15.602	0.56	0.47
$X_3 * X_4$	1	0.42	0.422	0.02	0.904
Error	12	336.53	28.044		
Lack-of-Fit	10	336.21	33.621	205.84	0.005
Error	2	0.33	0.163		
Total	26	1252.14			

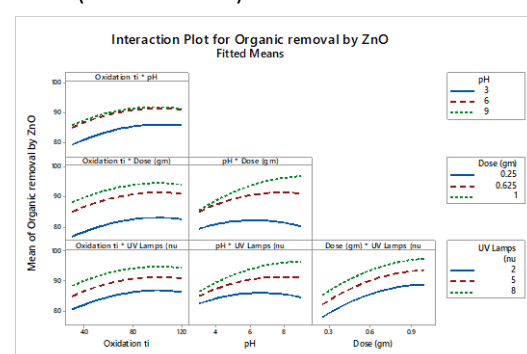
### 3.2. Statistical Analysis for photo oxidation

Twenty-seven statistically industrialized trials were intended to enhance and examine the integrated result of independent variables aimed at a specific group of process parameters. The independent variables for instance pH, dose, UV lamps, and oxidation time for Al<sub>2</sub>O<sub>3</sub>, TiO<sub>2</sub>, and ZnO treatments on the organic removal in produced water. The efficiency of photo-catalytic degradation in terms of organic removal under different operating conditions was presented in **Table 4**. Also, ANOVA examination for zinc oxide dose was tabulated in **Table 5**.

It can be seen from **Table 5**, the hybrid treatment of photo catalytic oxidation using ANOVA examination for zinc oxide dose displayed the findings for each parameter's Fisher value, P-test, adjusted sum of squares, adjusted mean of squares, degree of freedom, and sum of squares. The model's multiple correlation constant, which is 91.4% compatible with the regression's statistical significance, shows that only 14.11 percent of the total variants are not reinforced by work (Altunay *et al.* 2021).

The high capability response of removal with time of photo catalytic method conducted for all values of organic doses, without high concentrations dropped at a certain

period because of lacking passable places on the free radical from catalytic dose as presented in **Figure 5** interaction plot of variables of hybrid methods. Because the lines in these cells are convergent, the integrated properties of time, catalyst dose, and current had a significant contact focused on organic removal in wastewater. According to the results, the organic oxidation by zinc oxide is high removal compared with other catalysts amplified with dose, UV, pH and time, increasing from low to high. These core results are obvious in (Hu *et al.* 2016).

**Figure 5.** Interaction plot of variables.

The main effects of the problems were strong-minded, and the repercussions were analyzed using the "Minitab 17" software. The chief belongings of each limit on organic removal in wastewater are depicted in **Figure 6**. The dose, UV lamps, pH and time were the greatest significant variables touching organic removal in wastewater (Ali Abd Hassan & Shakir 2024).

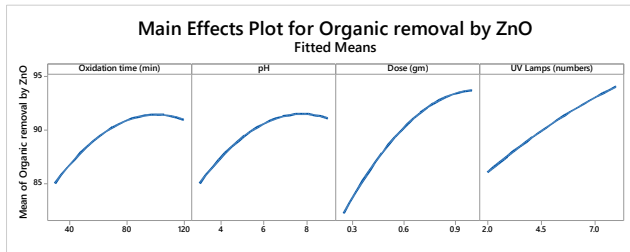


**Figure 6.** Main plot results for zinc oxide

### 3.2.1. The Effect of Catalyst Dose on Photo-Catalytic Degradation

The kind and dose of catalyst plays a major role on the efficiency of organic removal in photo-catalytic oxidation. In this work, the effect of catalyst dose on the organic removal was studied for ZnO, TiO<sub>2</sub>, Al<sub>2</sub>O<sub>3</sub> as shown in **Figure 7**. As can be seen from **Figure 7**, the organic removal was increased with an increasing in the catalyst dose from 65.2, 72.3 and 81.7% at 0.25 gm to the all-out elimination of 75.4, 79.4 and 88.4 % at 1 gm of catalyst dose Al<sub>2</sub>O<sub>3</sub> a TiO<sub>2</sub> and ZnO respectively (Ali A. Hassan & Al-Zobai 2019). It can be noticed also, varying the catalyst doses for each catalyst lead to different behavior of organic removal efficiency. It the high organic removal with higher catalyst doses can be attributed to the high active sites and high surface area produced which improve the catalytic degradation of organic in the produced water. Also, increase of catalyst amount is enhanced the reactivity and selectivity of catalytic materials towards removal of more pollutant from waste water. Based on the results obtained, it can be said that ZnO appeared the most effective catalyst with highest dose level obtained higher degradation efficiency (A T Nawaf & Hassan 2025).

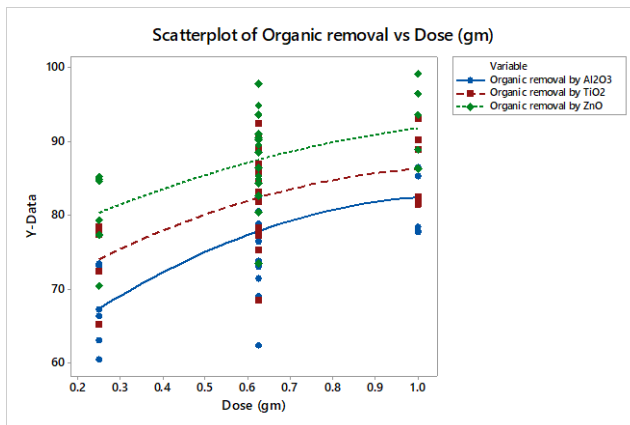


**Figure 7.** Effect of dose on the organic removal.

### 3.2.2. The Effect of Time on Photo-Catalytic Degradation

The effect of time on the photo-catalytic degradation of organic pollutant under ZnO, TiO<sub>2</sub>, Al<sub>2</sub>O<sub>3</sub> catalysts were conducted in the ranges (30-120 minute) as shown in

**Figure 8.** It was noticed that, from **Figure 8** the organic removal for ZnO catalyst was increased from 82% to 88% with increasing the time from 30 to 120 minute respectively. The same behavior with low organic removal was observed for catalyst TiO<sub>2</sub> and Al<sub>2</sub>O<sub>3</sub>. It can be concluded that 120 minute was the optimum level of time required for photo-catalytic degradation of organic removal within all kinds of catalysts. This can be attributed to the producing of free radicals along the time required that has the strong ability for the degradation of organic pollutant. Also, as time increased, reaction rate improved due to enhance the available period of the interactions and contact between reactants. This can be agreed with publication reported in literature (Alamery *et al.* 2023).

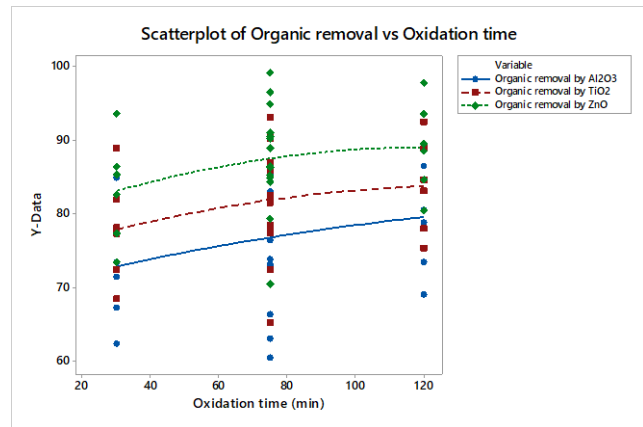


**Figure 8.** Effect of time on organic removal.

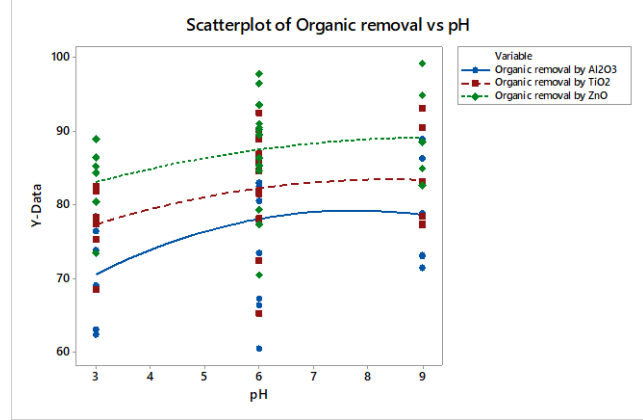


**Figure 9.** Effect of pH on organic elimination

### 3.2.3. The effect of pH on Photo-Catalytic Degradation

The photo catalytic process is meaningfully influenced by the value of pH then the finest performance of the method demands a preferred pH variety. In this work the effect of pH was conducted under various ranges (3-9) under 120 minute for each catalyst (ZnO, TiO<sub>2</sub>, Al<sub>2</sub>O<sub>3</sub>) was illustrated in **Figure 9**. The results obtained showed that for all catalyst types, that the organic removal was enhanced with increasing the solution pH. As seen in **Figure 9**, the organic removal under using ZnO catalyst enhanced higher organic removal directly when pH was increased from 3 to 9 (Amer T. Nawaf *et al.* 2025). The same trends with lower organic removal were seen for other catalysts (TiO<sub>2</sub>, Al<sub>2</sub>O<sub>3</sub>). Based on findings, it can be say that the pH of 9 was the optimum level required for

enhancing the organic removal. These clarifications conform to those of Ali *et al.* 2025 (A T Nawaf & Hassan 2025).

### 3.2.4. The Effect of UV lamps on Photo-Catalytic Degradation

UV Lamp can be considered a rate-controlling variable effect directly on the organic removal in photo-catalytic degradation. Different ranges of UV Lamps (2,6 and 8) was studied their effect on the organic removal in photo-catalytic degradation under different catalysts as shown in **Figure 10**. The other parameters of time and dosees kept constant. As shown in **Figure 10**, the UV Lamp has direct proportion with the organic removal for all types of catalyst. It is possible to see that the addition of more UV lamps increased removal efficiency; this energy boost causes titanium dioxide to produce more free radicals. The UV power has a direct impact on the catalyst's photo-catalytic rate. The photo-catalytic activity of the catalyst is limited at low UV light levels. The organic percent elimination rate rises as the incident power increases because the photo-catalytic process produces more free radicals. All of the available photons were used efficiently because it seems that the UV power measured in this study falls within the linear range.

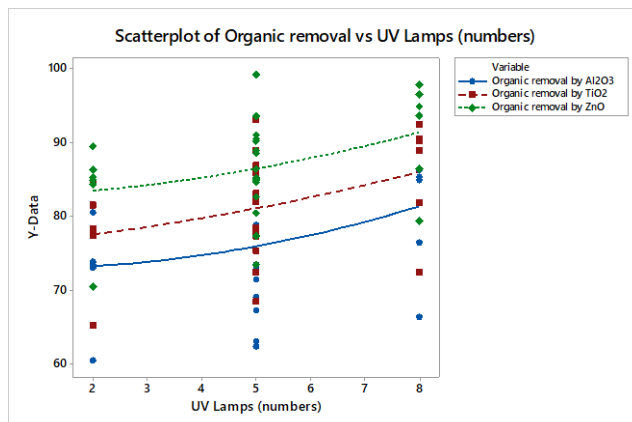


**Figure 10.** Effect of UV numbers on organic elimination

### 4. Enhancing the independent variables

Using Minitab-17, the finest values of independent variables, for instance, time, pH value, catalyst dose, and UV light, were used in the work. **Figure 11** clarify the effect of D-optimization. For the integrated treatment of photo catalytic oxidation, the best organic removal competencies were greater than 99 percent.

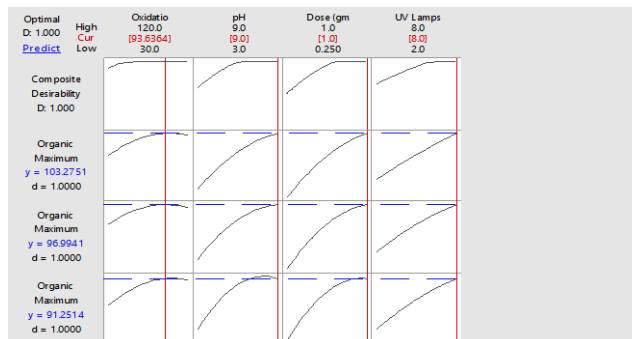


**Figure 11.** Finest independent variables with organic removal

### 5. Photo-Catalytic Degradation Kinetic

The kinetic of photo-catalytic degradation of organic removal was studied using ZnO catalyst experiments doses of (0.25,0.5 ,0.75 and 1 gm) due to the highest organic removal compared with other catalysts (TiO<sub>2</sub>, Al<sub>2</sub>O<sub>3</sub>) as show in **Figure 12**. The kinetic mode assumed pseudo first order model on ZnO catalyst results. The effect of catalyst doses on the rate constant was observed with plotting  $\ln(C_0/C)$  against time under each value of catalyst dose. By fitting the experiments, it was observed that the data well fitted with pseudo first order model. The pseudo-first order rate constant  $k_1$  ( $\text{min}^{-1}$ ) represents the slope of these figures, was calculated based on Eq (2). It can be seen from **Figure 12**, that with increasing the catalyst dose of ZnO from 0.25 g to 1 g, the rate constant increased directly from  $0.0019 \text{ min}^{-1}$  to  $0.003 \text{ min}^{-1}$  respectively. This was coinciding with Ali. *et al.* 2023 (Ibrahim *et al.* 2023) . The rate constants for ZnO catalyst were estimated and tabulated in **Table 6**. The ( $R^2$ ) coefficients were estimated as an indication for fitting these data. Where the closer one value indicated well fitted data. As seen from **Table 6**, the best fitted model that with  $R^2$  coefficient equal to 0.94 which is the closer to one compared to others.

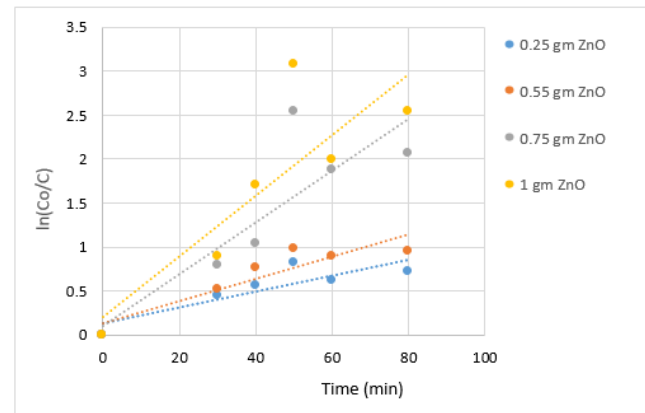


**Figure 12.** Pseudo-first order model for Photo-Catalytic Degradation using ZnO.

**Table 6.** The Pseudo-Rate constants for ZnO experiments.

ZnO	n=1	
	$k_1 \text{ min}^{-1}$	$R^2$
0.25	0.0019	0.91
0.5	0.002	0.33
0.75	0.003	0.94
1	0.0032	0.935

### 6. Economic Consideration of Wastewater

It is very important to take into account the economic consideration of wastewater treatment due to the large consumption and the high demands of large volumes of water in different sectors of industry fields such as petrochemicals, petroleum refinery, pharmaceuticals and food industry. The economic consideration of wastewater treatment management is very complex and beneficial for society obtaining more information's to guide investors and public policy to support improvements in wastewater management. Adequate wastewater collection,

treatment, and safe use or disposal can lead to significant environmental and health benefits. However, because some of these benefits do not have a market price, they have not traditionally been considered in the financial analysis of wastewater treatment projects, therefore underestimating total benefits. Many of authors pointed to the limitations of evaluation, narrowness and the simple assumptions into the version of cost benefits analysis (CBA) (Brouwer 2000). The economic analysis must compare the cost and benefits based on the environmental issues. Therefore, application of comprehensive CBA considered one of conditions for economic, social, environmental sustainability.

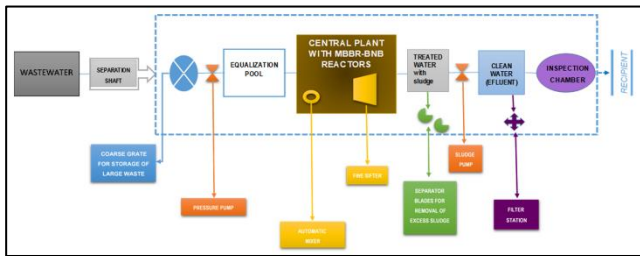


**Figure 13.** Process Flow Diagram of Variant V3 (Ćetković *et al.* 2022).

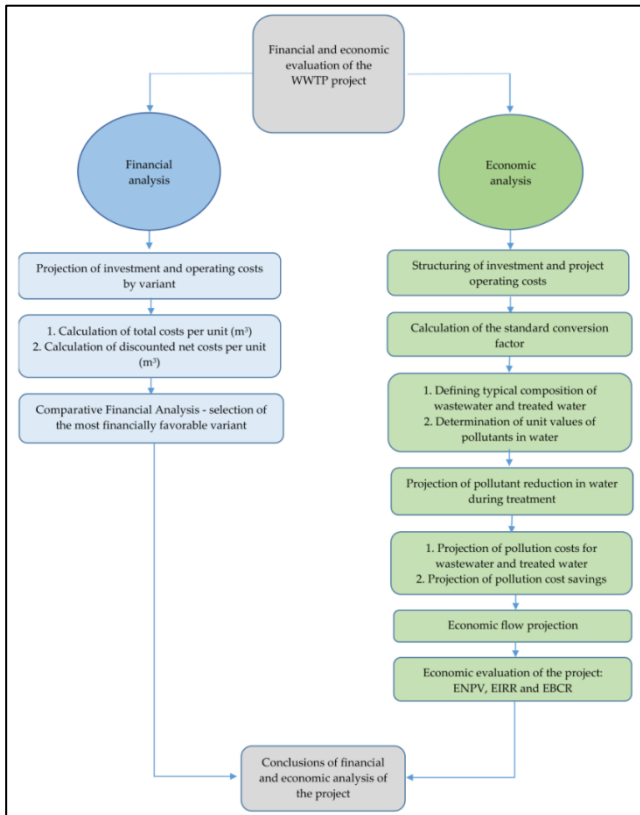


**Figure 14.** Methodological flowchart (Ćetković et al. 2022)

Additionally, in order to monetize the benefits of wastewater treatment projects, such as environmental and health benefits, other methods of assessing these benefits are being developed (Lienhoop *et al.* 2014) to overcome CBA constraints and include non-market benefits that are not easy to assess. Thus, guided by the importance of non-market benefits from projects of this type, some of the studies assessed the environmental benefits of using treated wastewater for various purposes

(Alcon *et al.* 2010; Birol *et al.* 2010). These results can be used more widely—in optimizing the WWTPs capacity and the exploitation of treated wastewater in agriculture as an alternative to groundwater (Lonigro *et al.* 2015; Lopez & Vurro 2008). Assessment of the economic and social costs and benefits in the CBA is also valuable in the process of deciding on the WWTP's size because certain research shows that different sizes of these plants have different economic and social justification. Another study was evaluated the economic and financial for variant V3 of wastewater treatment project in Nov Dojran, North Macedonia as illustrated in the process and methodology considered was illustrated in **Figure 13 and Figure 14** respectively. The main conclusions obtained were economic value about 16.38% from the economics of wastewater treatment.

Another benefit and economic analysis study on the energy saving and economic analysis of wastewater treatment focused on the large scale of wastewater treatment and re-used the outlet streams and get-benefit from the outlet heat in pre-heated the feed streams. (Mohammed *et al.* 2017), can provide an example study on the energy saving cost using heat exchangers and furnaces in order to reduce the overall energy consumption as shown in **Figure 15**. gPROMS software was simulated the mathematical model and validated the experimental results. It was observed based on the results obtained, designing a large scale for wastewater treatment required provided 25.21% cost saving and 43% energy saving (Mohammed *et al.* 2016, 2017).

In this study and according to authors reviewed, the results obtained before and after treatment can be give an indication of the economic of this study while achieving high conversion under low operating conditions and simple technique.

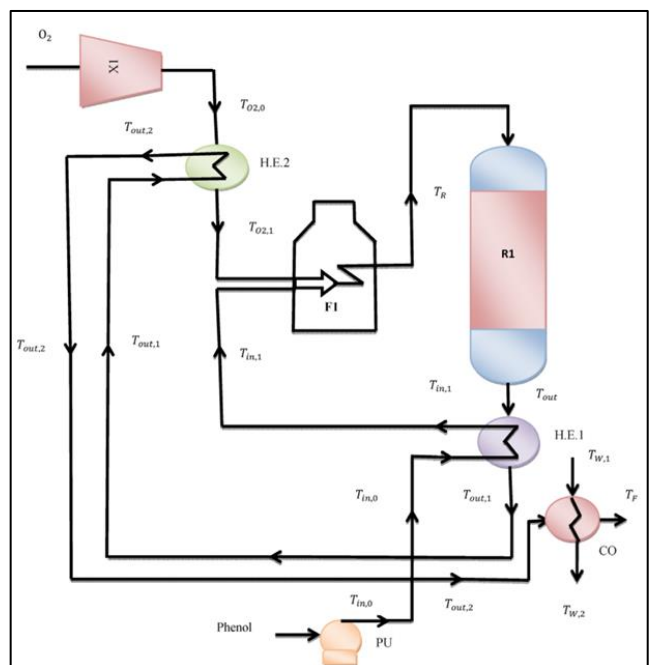


**Figure 15.** Schematic representation and energy saving of the process (Mohammed *et al.* 2017).

## 7. Conclusions

In this work, the organic removal from the produced water was conducted using photo-catalytic degradation under different levels operating conditions of time, pH, UV lamps and catalyst doses (ZnO, TiO<sub>2</sub> and Al<sub>2</sub>O<sub>3</sub>). Based on the results obtained, the highest value of organic removal achieved was 98.2%, 92.5% and 88.9% for ZnO, TiO<sub>2</sub> and Al<sub>2</sub>O<sub>3</sub> respectively. The optimum photo-catalytic degradation results achieved under optimum operating conditions of 120 minute, 9 pH, 1 g dose and 8 UV light for ZnO. This new treatment approach of produced waste water can be directly applied in the industrial fields due to it is cost effective, easily operated and highly efficient. The kinetics for photo-catalytic degradation was estimated for ZnO catalyst. It was revealed that the experimental data were well fitted with pseudo first order kinetic model. The kinetic parameters of the model estimated were 0.0032 min<sup>-1</sup> and 1pseudo-rate constant and pseudo first order respectively.

## Acknowledgment

This study done in Muthanna University-Iraq. The authors gratefully acknowledge the outstanding support provided by the technicians of the workshop in College of Engineering.

## References

Ahmed, I. H., Hassan, A. A., & Sultan, H. K. (2021). Study of Electro-Fenton Oxidation for the Removal of oil content in refinery wastewater. *IOP Conference Series: Materials Science and Engineering*, 1090(1), 012005. <https://doi.org/10.1088/1757-899x/1090/1/012005>

Anitha, A. S., et al. "Studies on kinetics, isothermal modelling and optimization of cow dung adsorbent for synthetic dairy wastewater treatment." *GLOBAL NEST JOURNAL* 26.10 (2024).

Al-Hassan, A. A., & Shakir, I. (2024). Enhanced Photocatalytic Activity of CuO/NCW via Adsorption Optimization for refinery wastewater. *Iranian Journal of Chemistry and Chemical Engineering, Articles in Press*.

Al-zobai, K. M. M., Hassan, A. A., & Kariem, N. O. (2020). Removal of amoxicillin from polluted water using UV/TiO<sub>2</sub>, UV/ZnO/TiO<sub>2</sub>, and UV/ZnO. *Solid State Technology*, 63(3), 3567–3575.

Alabdulla, W. M. S., Hamed, H. H., & Mohammed, A. E. (2020). Performance evaluation of combined O<sub>3</sub>/Fenton process on decolorization and COD removal of disperse blue 79 dye from aqueous solution. *Desalination and Water Treatment*, 173, 420–426.

Alamery, H. R. D., Hassan, A. A., & Rashid, A. H. (2023). Copper Removal in Simulated Wastewater by Solar Fenton Oxidation. *AIP Conference Proceedings*, 2806(1). <https://doi.org/10.1063/5.0167259>

Alcon, F., Pedrero, F., Martin-Ortega, J., Arcas, N., Alarcon, J. J., & De Miguel, M. D. (2010). The non-market value of reclaimed wastewater for use in agriculture: a contingent valuation approach. *Spanish Journal of Agricultural Research*, 8, 187–196.

Altunay, S., Kılıç, H., Öden, M. K., & Çakmak, B. (2021). Pollutant removal from mining processing wastewater by electrochemical method. *Global Nest Journal*, 23(2), 178–185. <https://doi.org/10.30955/gnj.003683>

Alturki, S. F., Ghareeb, A. H., Hadi, R. T., & Hassan, A. A. (2021). Evaluation of Using Photovoltaic Cell in the Electro-Fenton Oxidation for the Removal of Oil Content in Refinery Wastewater. *IOP Conference Series: Materials Science and Engineering*, 1090(1), 012012. <https://doi.org/10.1088/1757-899x/1090/1/012012>

Atiyah, A. S., Al-Samawi, A. A. A., & Hassan, A. A. (2020). Photovoltaic cell electro-Fenton oxidation for treatment oily wastewater. *AIP Conference Proceedings*, 2235(May). <https://doi.org/10.1063/5.0008937>

Birol, E., Koundouri, P., & Kountouris, Y. (2010). Assessing the economic viability of alternative water resources in water-scarce regions: Combining economic valuation, cost-benefit analysis and discounting. *Ecological Economics*, 69(4), 839–847.

Brouwer, R. (2000). Environmental value transfer: state of the art and future prospects. *Ecological Economics*, 32(1), 137–152.

Cetković, J., Knežević, M., Lakić, S., Žarković, M., Vučadinović, R., Živković, A., & Cvijović, J. (2022). Financial and economic investment evaluation of wastewater treatment plant. *Water*, 14(1), 122.

El-Hendawy, A. N. A. (2006). Variation in the FTIR spectra of a biomass under impregnation, carbonization and oxidation conditions. *Journal of Analytical and Applied Pyrolysis*, 75(2), 159–166.

Gutiérrez-Mata, A. G., Velázquez-Martínez, S., Álvarez-Gallegos, A., Ahmadi, M., Hernández-Pérez, J. A., Ghanbari, F., & Silva-Martínez, S. (2017). Recent Overview of Solar Photocatalysis and Solar Photo-Fenton Processes for Wastewater Treatment. *International Journal of Photoenergy*, 2017. <https://doi.org/10.1155/2017/8528063>

Hassan, Ali A., & Al-Zobai, K. M. M. (2019). Chemical oxidation for oil separation from oilfield produced water under uv irradiation using titanium dioxide as a nano-photocatalyst by batch and continuous techniques. *International Journal of Chemical Engineering*, 2019. <https://doi.org/10.1155/2019/9810728>

Hassan, Ali A., Naeem, H. T., & Hadi, R. T. (2019). A Comparative Study of Chemical Material Additives on Polyacrylamide to Treatment of Waste Water in Refineries. *IOP Conference Series: Materials Science and Engineering*, 518(6), 62003. <https://doi.org/10.1088/1757-899X/518/6/062003>

Hassan, Ali Abd, & Shakir, I. K. (2024). Synthesis of Nanocellulose Using Ultrasound - Assisted Acid Hydrolysis for Adsorption/Oxidation of Organic Pollutants in Wastewater Under Uv and Solar Light. *Journal of Sustainability Science and Management*, 19(12), 120–140. <https://doi.org/10.46754/jssm.2024.12.008>

Hassan, Ali Abed, & Shakir, I. K. (2024). Kinetic Insights into Solar-Assisted Fabrication and Photocatalytic Performance of CoWO<sub>4</sub>/NCW Heterostructure. *Bulletin of Chemical Reaction Engineering & Catalysis*, 10.

Hu, X., Wang, H., & Liu, Y. (2016). Statistical Analysis of Main and Interaction Effects on Cu(II) and Cr(VI) Decontamination by Nitrogen-Doped Magnetic Graphene Oxide. *Scientific Reports*, 6(September), 1–11. <https://doi.org/10.1038/srep34378>

Ibrahim, H. A., Hassan, A. A., Ali, A. H., & Kareem, H. M. (2023). Organic removal from refinery wastewater by using electro catalytic oxidation. *AIP Conference Proceedings*, 2806(1).

Ibrahim, M. K., Al-Hassan, A. A., & Naje, A. S. (2019). Utilisation of cassia surattensis seeds as natural adsorbent for oil content removal in oilfield produced water. *Pertanika Journal of Science and Technology*, 27(4), 2123–2138.

Issa, Y. S., Mahmood, Q. A., Humadi, J. I., Hassan, G., & Haldhar, R. (2025). Design of New Wet Heterogeneous Photo Oxidation Process for Refinery Waste Water Treatment in Photo Baffled Reactor. *Water, Air, & Soil Pollution*, 236(1), 70. [doi.org/10.1007/s11270-024-07706-0](https://doi.org/10.1007/s11270-024-07706-0)

Ivanenko, O., Shabliy, T., & Nosachova, Y. (2020). Application of potassium ferrate in water treatment processes. *Journal of Ecological Engineering*, 21(7), 134–140. <https://doi.org/10.12911/22998993/125438>

Kamal, S. K., Mohammed, A. E., Alabdaba, W. M., Hamed, H. H., & Waly, K. A. (2020). Industrial Wastewater Treatment in North Gas Company By Using Coagulation–Flocculation Process. *Journal of Petroleum Research and Studies*, 10(4), 252–269.

Khamees, L. A., Humadi, J. I., Aqar, D. Y., Aabid, A. A., Ahmed, M. A., Hameed, M. B., & Ahmed, M. A. (2023). Improvement of the activity of a new nano magnetic titanium catalyst by using alkaline for refinery wastewater oxidation treatment in a batch baffled reactor. *Journal of Water Process Engineering*, 56, 104537. <https://doi.org/10.1016/j.jwpe.2023.104537>

Lienhoop, N., Al-Karablieh, E. K., Salman, A. Z., & Cardona, J. A. (2014). Environmental cost–benefit analysis of decentralised wastewater treatment and re-use: a case study of rural Jordan. *Water Policy*, 16(2), 323–339.

Lonigro, A., Montemurro, N., Rubino, P., Vergine, P., & Pollice, A. (2015). Reuse of treated municipal wastewater for irrigation in Apulia region: the "In. Te. RRA" project. *Environmental Engineering & Management Journal (EEMJ)*, 14(7).

Lopez, A., & Vurro, M. (2008). Planning agricultural wastewater reuse in southern Italy: The case of Apulia Region. *Desalination*, 218(1–3), 164–169.

Mohammadi Ziarani, G., Rezakhani, M., Feizi-Dehnayebi, M., & Nikolova, S. (2024). Fumed-Si-Pr-Ald-Barb as a Fluorescent Chemosensor for the Hg<sup>2+</sup> Detection and Cr<sup>2072-</sup> Ions: A Combined Experimental and Computational Perspective. *Molecules*, 29(20), 4825.

Mohammed, A. E., Hamed, H. H., Alabdaba, W. M. S., & Ali, O. M. (2019). COD removal from disperse blue dye 79 in wastewater by using Ozone-Fenton process. *IOP Conference Series: Materials Science and Engineering*, 518(6), 62015.

Mohammed, A. E., Jarullah, A. T., Gheni, S. A., & Mujtaba, I. M. (2016). Optimal design and operation of an industrial three phase reactor for the oxidation of phenol. *Computers & Chemical Engineering*, 94, 257–271. [https://doi.org/https://doi.org/10.1016/j.compchemeng.2016.07.018](https://doi.org/10.1016/j.compchemeng.2016.07.018)

Mohammed, A. E., Jarullah, A. T., Gheni, S. A., & Mujtaba, I. M. (2017). Significant cost and energy savings opportunities in industrial three phase reactor for phenol oxidation. *Computers & Chemical Engineering*, 104, 201–210. <https://doi.org/https://doi.org/10.1016/j.compchemeng.2017.04.016>

Naeem, H. T., Hassan, A. A., & Al-Khateeb, R. T. (2018). Wastewater-(Direct red dye) treatment-using solar fenton process. *Journal of Pharmaceutical Sciences and Research*, 10(9), 2309–2313.

Nawaf, A. T., Humadi, J. I., Jarullah, A. T., Ahmed, M. A., Hameed, S. A., & Mujtaba, I. M. (2023). Design of nano-catalyst for removal of phenolic compounds from wastewater by oxidation using modified digital basket baffle batch reactor: Experiments and modeling. *Processes*, 11(7), 1990. <https://doi.org/10.3390/pr11071990>

Nawaf, A. T., & Hassan, A. A. (2025). Design of (MnO<sub>2</sub>/GO) for removal organic compounds from wastewater using digital baffle batch reactor. *International Journal of Environmental Science and Technology*, 1–20.

Nawaf, Amer T., Humadi, J. I., Hassan, A. A., Habila, M. A., & Haldhar, R. (2025). Improving of fuel quality and environment using new synthetic (Mn<sub>3</sub>O<sub>4</sub>/AC-nano-particles) for oxidative desulfurization using digital baffle batch reactor. *South African Journal of Chemical Engineering*, 52(November 2024), 8–19. <https://doi.org/10.1016/j.sajce.2025.01.003>

Ohara, C., Hongo, T., Yamazaki, A., & Nagoya, T. (2008). Synthesis and characterization of brookite/anatase complex thin film. *Applied Surface Science*, 254(20), 6619–6622.

Orooji, N., Takdastan, A., Jalilzadeh Yengejeh, R., Jorfi, S., & Davami, A. H. (2020). Photocatalytic degradation of 2, 4-dichlorophenoxyacetic acid using Fe<sub>3</sub>O<sub>4</sub>@ TiO<sub>2</sub>/Cu<sub>2</sub>O magnetic nanocomposite stabilized on granular activated carbon from aqueous solution. *Research on Chemical Intermediates*, 46(5), 2833–2857.

Saleh Jafer, A., & Hassan, A. A. (2019). Removal of oil content in oilfield produced water using chemically modified kiwi peels as efficient low-cost adsorbent. *Journal of Physics: Conference Series*, 1294(7). <https://doi.org/10.1088/1742-6596/1294/7/072013>

Sh, A. W. M. (2020). Decolourization of Disperse Red 17 Dye from Wastewater by Using Coagulation/Flocculation Process. *Indian J. Environmental Protection*, 40(8), 841–846.

Srivastava, V. C., Mall, I. D., & Mishra, I. M. (2006). Equilibrium modelling of single and binary adsorption of cadmium and nickel onto bagasse fly ash. *Chemical Engineering Journal*, 117(1), 79–91.

Ulhaq, I., Ahmad, W., Ahmad, I., Yaseen, M., & Ilyas, M. (2021). Journal of Water Process Engineering Engineering TiO<sub>2</sub> supported CTAB modified bentonite for treatment of refinery wastewater through simultaneous photocatalytic oxidation and adsorption. *Journal of Water Process Engineering*, 43(May), 102239. <https://doi.org/10.1016/j.jwpe.2021.102239>

Zhang, Y., Li, Z., Gong, C., Lv, X., Kong, D., & Chen, X. (2024). Optimization of the Freeze Crystallization Process for Recovering of Copper (II) Sulphate from Electroplating Wastewater Using Response Surface Methodology (RSM). *GLOBAL NEST JOURNAL*, 26(9).

Zawadzki, J. (1989). Infrared spectroscopy in surface chemistry of carbons. *Chemistry and Physics of Carbon*, Vol. . Marcel Dekker, New York, 21, 147–386.